

3 CAESAR (Cellular Automata Evolutionary Slope And River Model)

Murray and Paola's model has inspired the development of a series of similar CM. After the development of a basin evolution LEM (Landscape Evolution Model), Coulthard continued in the refinement of the same model, adapted for applications in river beds, of any morphology, as described in Coulthard et al. (2000, 2002, 2007), Coulthard et al. (2008), Coulthard (2006), and Van De Wiel et al. (2007). His model was built editing the MP routing scheme: he honed modules calculation of tie rods for water and sediment, and developed algorithms for process simulation of bank erosion and transport in suspension. The Coulthard's model, called CAESAR (Cellular Automation Evolutionary Slope And River Model) was applied to river stretches from 4 to 40 km, with a cell size of calculation variables from 2 m × 2 m, up to 50 m × 50 m. Used in reach mode (a section of the river), the model requires several input data: the starting DEM, the values of both solid and liquid flow in input from upstream, particle size, characterization of the background texture and the possible vegetation cover. For each cell of the calculation model it associates a dimension value, the liquid flow, specific particle size, the vegetation cover and the thickness of the erodible riverbed. CAESAR implements an iterative process of "scanning" updating the set of values associated with each cell, by the application of all the rules that govern the simplified individual processes. Generally we can distinguish 5 sets of rules:

1. hydraulic – it regulates the distribution of liquid flow;
2. fluvial erosion and deposition – for modelling the bed load transport in suspension as reported in Wilcock and Crowe (2003) and Einstein (1950);
3. bank erosion – it defines the processes of retraction of river banks only for cells close to the active edge of the riverbed;
4. hydrological – it regulates the conversion inflows–outflows adopting TOPMODEL as basic scheme as in Beven and Kirkby (1979);

837

5. slope processes (mass movement, creep) – it models the handling of the collapsing soil or creep from the slopes.

CAESAR, applied in reach mode, implements only the cellular automation of liquid components (1), sediment transport (2), and lateral erosion (3). For each iteration CAESAR changes the values of the cell analyzed, during the previous time step, in accordance with the set of rules listed above and with the property values of neighboring cells. This means that the total amount of erosion of a cell depends on the water head on that cell and by the slope between the same cells and the adjacent ones. CAESAR can work both in basin scale and in riverbed scale; the input needed for a basin scale analysis is the hourly rain, constant throughout the basin which then becomes flow according to the rainfall-runoff TOPMODEL modified model as shown in Fig. 1.

Wishing to use CAESAR for a section-scale, the input required by the model is the flow rate (solid and liquid). For each scan (scanning and updating the values of all cells in a given area for a given time step) the hydraulic flow (both in riverbed scale and in basin scale) is directed to the three cells hydraulically lower but, if the total water flow is greater than the subsurface flow, the excess is treated as runoff and its swing is evaluated through an +adaptation of the Manning's equation as shown in Eq. (1):

$$Q = UA = (h^{2/3} \sqrt{SA}) \quad (1)$$

where Q , U and h represent respectively the flow rate, the flow velocity and the water head, A is the area of the cross section of the flow, S is the slope. For cells interested, a sash evaluation is obtained through the equation reported in Wilcock and Crowe (2003), applied to eleven different granulometric fractions (1 to 256 mm) that defines the particle size of the riverbed, in turn divided into a series of 10 active layers, according to Hoey and Ferguson (1994). Depending on the size, the different clusters are transported both as load and as suspended bottom sediments, determining the creation of an "armored" surface and a stratification of the bed. When simulations are very long, it is necessary to be sure that the finer sediments are deposited in order

838

subject, in such parts, to instability phenomena for landslide erosion. Recent studies, as described in Surian et al. (2008, 2009a, b), have shown that impressive concordances and some specific exceptions in the behaviour of these watercourses, may constitute a group sufficiently representative of the changes undergone by most of the main Italian rivers. Various forms of human intervention have affected the water courses, with different impacts and timing, but substantially with similar morphological manifestations. Sewer, sediment extraction, dams construction, reforestation, have changed, directly or indirectly, the morphological dynamics in all these contexts. In many cases the embankments construction or repellents bank began at the end of XIX century and has lasted up to the present.

Reforestation and mountain renovations are not well documented, but the available data suggest that both of these forms of intervention have been undertaken with effect from the 1920s–1930s. Even the big artificial dams had considerable momentum after the First World War, and later in the 1950s and 1960s. Finally the sediment extraction, corresponded to a period of forty years, from 1950 to 1990, during which millions of cubic meters of sediment were removed from the main Italian watercourses. These interventions have dramatically altered the regime of sediments, and still, in spite of the situation in recent years has substantially improved, the consequences of so strong interventions are difficult to quantify, monitor and predict. More specifically, in this study, CAESAR regards the application of the model to a particular waterway, the Aniene River. This choice derives from evaluations taking into account the availability of good data, the characteristics of the Aniene basin, the predominance of morphology braided channels within the case study and the morphological evolution that have distinguished the basin in the short and medium term. The rains have an intensity peak in November and a minimum in July. The 60 % of the rains fall during the autumn–winter and only 10 % during the summer. In fact, precipitation values of 1400 mm per year are registered on Albani Hills, Cimini Hills and Amiata Massif. Extent of precipitation slightly higher has been observed in the Appennine dorsal: 1500 mm per year on the Sibillini and Tiburtini Hills, 1600 mm on on Reatini and Simbruini Hills that drains towards the

843

Aniene. Maximum precipitation of one or more consecutive days is very important in the formation of floods. Hydrographic service data related to 1921–1970 show that the maximum daily rainfall with a duration that goes from one to five consecutive days for all stations ranges between 374 and 534 mm. In conclusion we can say that the conditions for an exceptional state occur when there is a close succession of preparatory precipitations and a determinant precipitation. Preparatory precipitations occur in the two or three months before the determinant precipitation, which occurs only two or three days before the ridge of full.

6 New functionalities added

Additional functionality has been added with the intent of being able to compare the results obtained with the simulation of flooding and possible map obtained by other software. In particular, it is possible to display a static image that represents the same area examined during the simulation in which you highlight the areas of the flooding theatre. All this has been made possible by adding a specific menu item called “Load Image” in the main bar of the commands as shown in Fig. 5, by mean of which it is possible to reach an initially empty window that allows to select an appropriate image as shown in Fig. 6 (the result of a previous processing, as mentioned above).

With the help of this additional functionality, it is possible to pursue new and very important objectives, as shown in Fig. 7:

1. check the real dynamics of flooding;
2. validate the simulation ended with the image obtained by digital processing;
3. obtain a further estimation of the possible flooding extension.

844

7 Objectives

This research aims to apply the CAESAR model to a stretch of the Aniene River and to characterize the mapping of the flood boundaries. In addition, a comparison will be made with an existing and well known Open Source Earth Observation System: Next
 5 ESA SAR Toolbox (NEST version 4C-1.1). In fact, the principle of using radar for flood mapping is that the intensity of the radar backscattered signal depends on the roughness of the surface it interacts with. Water bodies generally create a very quiet (unless strong winds induce waves) and homogeneous surface. Therefore the incident, side
 10 looking, radar pulse will be scattered away from the radar sensor (specular reflection) and the radar image over that area will be black, or very dark due to little return of the radar pulse. The surrounding rough land surface will be much brighter, due to higher return, thereby distinguishing it from the water surface. In order to identify flooded areas from permanent water bodies, an image acquired during the flood needs to be compared with another image acquired when there was no flood. It is necessary to extract
 15 both images through the same sensor geometry. This is because the brightness of the radar return depends on the angle and direction of the incident radar pulse.

8 Flood water extraction from RADARSAT images

Remote Sensing with Optical sensor depends on sunlight illuminating the Earth in order to obtain useful imagery. Its performance is limited by the presence of clouds, fog, smoke or darkness. However, RADARSAT does not have such limitations. At the heart
 20 of RADARSAT there is an advanced radar sensor called Synthetic Aperture Radar (SAR). SAR is a microwave instrument that sends pulsed signals to Earth and processes the received reflected pulses. The SAR technology based on RADARSAT sensors provides its own microwave illumination and thus operates day or night, regardless
 25 of weather conditions. Spaceborne and airborne SAR imagery used in flood mapping can be broadly defined as low (about 100 m), medium (10–25 m) and high (1–2 m)

845

spatial resolutions as in Di Baldassarre et al. (2011). Mapping of water surface using SAR is possible because the SAR backscatter is very low due to the specular reflection as shown in Fig. 8 when the water surface is smooth. As a result, flooded areas appear
 5 as dark tones due to the low backscattering response whereas land surface appear as bright tones because the rough soil surface and vegetation produce diffused reflection resulting in a strong backscatter. This tonal variation according to the backscatter response in SAR images can be used to separate water from soil.

The four common steps for a flood mapping area procedure are:

- visual interpretation;
- 10 – histogram thresholding;
- active contour;
- image texture variance.

In visual interpretation, flooded area is represented by a visual digitizing method, whereas in histogram thresholding, the optimal gray threshold is used to individuate
 15 flooded areas. Active contour model delineates the flood extent based on dynamic curvilinear contours to search the edge image space until it settles upon image region boundaries. In image texture method, tonal changes may be modeled as a gray level function using statistical methods on the image histogram as in Schumann et al. (2009). However, no single method can be seen as the most appropriate for all the images and
 20 all methods are not equally good for a particular type of image. An overview of the research methodology is seen in Fig. 9:

the previous flow chart was obtained by the following operations in NEST:

- Creation of the project file and opening the data: both acquired images were used
 25 to map the flooding event. One image was taken during the floods, known as the “crisis image” while the second image, known as the “archive image”, is covering approximately the same area.

846

- View metadata: here is stored the information taken from the metadata files, including the mission, product type, acquisition date and time, track and orbit.
- View geographical coverage of both images: a map will show the footprints of the images calculated from the metadata.
- 5 – View and crop the images: inspecting both the images, we focus on the extensive dark area of the crisis image. This is the area of flooding and we are interested only in the part of the images where the flood are visible. Cropping the images to include only this area will save much computation time.
- Orthorectification of the images with a DEM.
- 10 – Create a stack and compare images: in order to compare the two images we stack them together and view them in the same viewer. We then create a 3 color composite image and inspect the changes between the two acquisition times. In order to enhance the differences between the archive and crisis image in one layer we will create an RGB image view. To do this, first we need to ensure that there are 3 channels from which an RGB image can be created. This combination will enable us to differentiate between areas that are flooded and permanent water bodies. In areas that are flooded, the red channel will be dark but the green and blue channels will be bright, therefore the pixels should appear bright cyan. A permanent water bodies will be dark in all the channels. All other areas will display a shade of gray as the backscatter intensity should be the same. However, in this case the images are not from the same track, therefore there will be greater differences between the backscattered images even in areas where they should be the same (due to the different viewing angles).
- 15 – Save RGB image view as a KMZ file: once the file is saved we can watch it in Google Heart overlaying streets and places names onto the image to see which areas are flooded.
- 20
- 25

847

- Calculation of flooded area: we try to quantify the magnitude of the floods. To do this we need to know the number of flooded pixels. The first step is to define thresholds for the pixel values in both images where the flood is present. Good threshold values for flooded areas could be < 800 for the crisis image and > 900 for the archive icon. This will mask flooded pixels, without classifying permanent water bodies as flooded areas. To mask only the flooded area and to avoid the edges containing regions not covered by both images, we will utilize the mask only to the function where both images overlap. Knowing the size of the image pixel (see range spacing and azimuth spacing in metadata) and knowing how many pixels are masked as flood, it is possible to calculate the size of the affected area.
- 5
- 10

9 Conclusions

Numerical modeling is undoubtedly a tool with interesting application perspectives in fluvial geomorphological contexts, in particular the so called “Reduced Complexity Models” and among them the “Cellular Model”. In the specific context of this research, the CAESAR model, widely described also in Coulthard et al. (1999), is applied to a stretch of the Aniene River with the overall objective to fully characterize the developments of the last 40yr and then to obtain a quantitative evaluation about its evolutionary trend in the short and medium term. CAESAR, in fact, has been developed mainly to study the geomorphological changes in catchment or riverbed for long time periods (hundreds years). CAESAR is a quantitative model that is currently mainly used for research purposes. The correctness of simulations, however, have been tested essentially from a qualitative point of view. The results obtained, related to erosion/depositions, and to the water head (connected to the channel configuration of lean) are congruent. In conclusion, we can say that CAESAR reproduces realistic results, at least qualitatively, even for studying the effects on the dynamics of riverbed, due to the presence of hydraulic works. It would be interesting, deepening the quantitative aspect; to do this we need to find a consistent amount of data on bathymetry,

848

profiles, distribution particle size, liquid and solid flow, spread over a time interval sufficiently large and in different morphological and different beds.

Acknowledgements. I would like to especially thank F. Del Frate and M. Ioannilli for supporting me and all colleagues in the Earth Observation Laboratory (Department of Civil Engineering and Computer Science, Tor Vergata University) for providing various images for this research.

References

- Beven, K.: Linking parameters across scales: subgrid parameterizations and scale dependent hydrological models, *Hydrol. Process.*, 9, 507–525, 1995. 840
- Beven, K. and Kirkby, M.: A physically based, variable contributing area model of basin hydrology/Un modèle à base physique de zone d'appel variable de l'hydrologie du bassin versant, *Hydrolog. Sci. J.*, 24, 43–69, 1979. 837, 840
- Beven, K. and Wood, E. F.: Catchment geomorphology and the dynamics of runoff contributing areas, *J. Hydrol.*, 65, 139–158, 1983. 840
- Beven, K., Lamb, R., Quinn, P., Romanowicz, R., and Freer, J.: TOPMODEL, *Comput. Model. Watershed Hydrol.*, edited by: Singh, V. P., Water Resources Publications, Boulder, CO, Chap. 18, 627–668, 1995. 841
- Castiglioni, G. B.: *Geomorfologia*, Utet, Torino, 436 pp., 1982. 834
- Coulthard, T., Wiel, M., and Van De, J.: A cellular model of river meandering, *Earth Surf. Proc. Land.*, 31, 123–132, 2006. 837, 841
- Coulthard, T., Kirkby, M., and Macklin, M. G.: *Modelling the Impacts of Holocene Environmental Change in an Upland River Catchment, Using a Cellular Automaton Approach*, John Wiley and Sons, Chichester, 1999. 848
- Coulthard, T., Kirkby, M., and Macklin, M.: Modelling geomorphic response to environmental change in an upland catchment, *Hydrol. Process.*, 14, 2031–2045, 2000. 837
- Coulthard, T., Macklin, M., and Kirkby, M.: A cellular model of Holocene upland river basin and alluvial fan evolution, *Earth Surf. Proc. Land.*, 27, 269–288, 2002. 837
- Coulthard, T., Hicks, D., and Van De Wiel, M. J.: Cellular modelling of river catchments and reaches: advantages, limitations and prospects, *Geomorphology*, 90, 192–207, 2007. 837
- Coulthard, T., De Rosa, P., and Marchesini, I.: CAESAR: un modello per la simulazione delle dinamiche d'alveo, *Il Quaternario*, 21, 207–214, 2008. 836, 837

849

- De Rosa, P.: Un approccio modellistico per il fenomeno delle occlusioni d'alveo per frane: una modifica al modello CAESAR, *Giornale di Geologia Applicata*, 8, 277–284, 2008. 842
- Di Baldassarre, G., Schumann, G., Brandimarte, L., and Bates, P.: Timely low resolution SAR Imagery to support floodplain modelling: a case study review, *Surv. Geophys.*, 32, 255–269, 2011. 846
- Einstein, H. A.: *The bed-load function for sediment transportation in open channel flows*, 1026, US Department of Agriculture, Washington, D.C., United States, 1950. 837
- Formann, E., Habersack, H., and Schober, S.: Morphodynamic river processes and techniques for assessment of channel evolution in Alpine gravel bed rivers, *Geomorphology*, 90, 340–355, 2007. 835
- Hoey, T. B. and Ferguson, R.: Numerical simulation of downstream fining by selective transport in gravel bed rivers: model development and illustration, *Water Resour. Res.*, 30, 2251–2260, 1994. 838
- Lane, S., Bradbrook, K., Richards, K., Biron, P., and Roy, A.: The application of computational fluid dynamics to natural river channels: three-dimensional versus two-dimensional approaches, *Geomorphology*, 29, 1–20, 1999. 835
- Li, S., Millar, R., and Islam, S.: Modelling gravel transport and morphology for the Fraser river gravel reach, British Columbia, *Geomorphology*, 95, 206–222, 2008. 835
- Marchetti, M.: *Geomorfologia Fluviale*, Pitagora edn., Bologna, 2000. 834
- Montoya Cardona, M. M.: *Analisi dinamica-morfologica dei corsi d'acqua pseudo meandriciformi mediante modelli a fondo mobile*, Tesi di Dottorato in Idronomia Ambientale, Università degli studi di Padova, Padova, 2008. 835
- Murray, A. B. and Paola, C.: A cellular model of braided rivers, *Nature*, 371, 54–57, 1994. 836
- Murray, A. B. and Paola, C.: Properties of a cellular braided-stream model, *Earth Surf. Proc. Land.*, 22, 1001–1025, 1997. 836
- Murray, A. B. and Paola, C.: Modelling the effect of vegetation on channel pattern in bedload rivers, *Earth Surf. Proc. Land.*, 28, 131–143, 2003. 836
- Newson, M. and Sear, D.: River conservation, river dynamics, river maintenance: contradictions, in: *Conserving our Landscape Joint Nature Conservancy*, edited by: White, S., Green, J., and Macklin, M. G., Peterborough, UK, 139–146, 1993. 834
- Nicholas, A. P.: Cellular modelling in fluvial geomorphology, *Earth Surf. Proc. Land.*, 30, 645–649, 2005. 835

- Quinn, J. M., Coleman, R. J., Macmillan, S., and Barraclough, D. R.: The 1995 revision of the joint US/UK geomagnetic field models, II: Main field, *J. Geomagn. Geoelectr.*, 49, 245–261, 1997. 840
- Schumann, G., Bates, P. D., Horritt, M. S., Matgen, P., and Pappenberger, F.: Progress in integration of remote sensing – derived flood extent and stage data and hydraulic models, *Rev. Geophys.*, 47, RG4001, doi:10.1029/2008RG000274, 2009. 846
- 5 Surian, N., Ziliani, L., Cibien, L., Cisotto, A., and Baruffi, F.: Variazioni morfologiche degli alvei dei principali corsi d'acqua veneto-friulani negli ultimi 200 anni, *Il Quaternario*, 21, 279–290, 2008. 843
- 10 Surian, N., Rinaldi, M., Pellegrini, L., Audisio, C., Maraga, F., Teruggi, L., Turitto, O., and Ziliani, L.: Channel adjustments in northern and central Italy over the last 200 years, *Geol. S. Am. S.*, 451, 83–95, 2009a. 843
- Surian, N., Ziliani, L., Comiti, F., Lenzi, M. A., and Mao, L.: Channel adjustments and alteration of sediment fluxes in gravel-bed rivers of North-Eastern Italy: potentials and limitations for channel recovery, *River Res. Appl.*, 25, 551–567, 2009b. 843
- 15 Van De Wiel, M. J., Coulthard, T. J., Macklin, M. G., and Lewin, J.: Embedding reach-scale fluvial dynamics within the CAESAR cellular automaton landscape evolution model, *Geomorphology*, 90, 283–301, 2007. 837
- Wilcock, P. R. and Crowe, J. C.: Surface-based transport model for mixed-size sediment, *J. Hydraul. Eng.*, 129, 120–128, 2003. 837, 838
- 20 Wolfram, S.: Universality and complexity in cellular automata, *Physica D*, 10, 1–35, 1984. 836

851

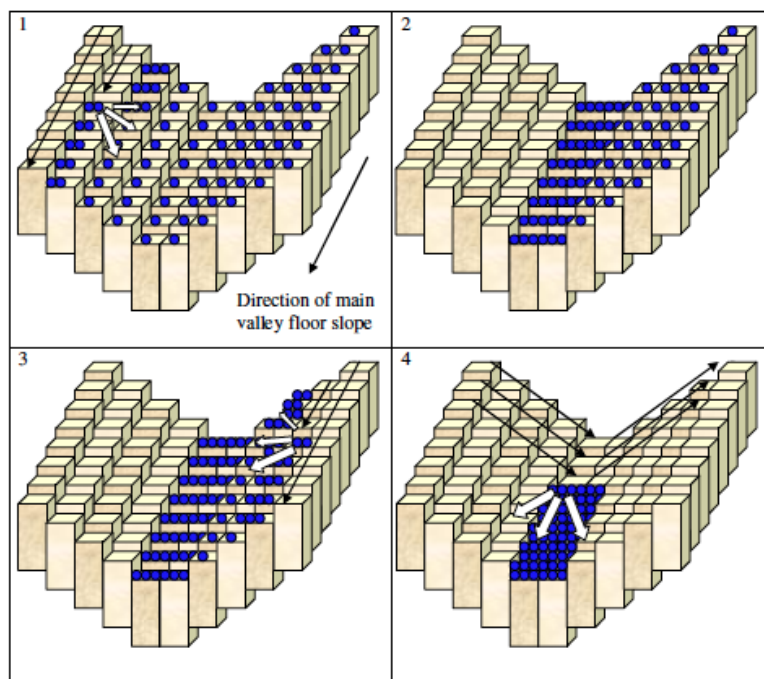


Fig. 1. Schematic diagram of the CAESAR scanning flow routing algorithm.

852

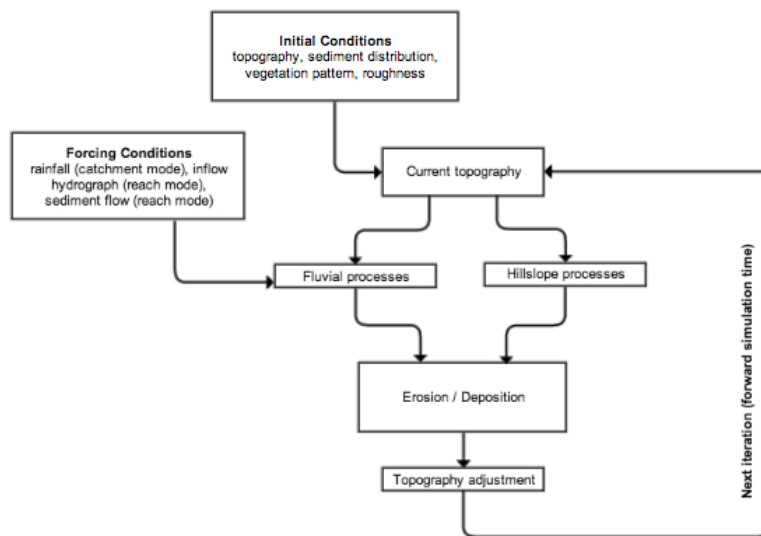


Fig. 2. Schematic of CAESAR's operation.

853

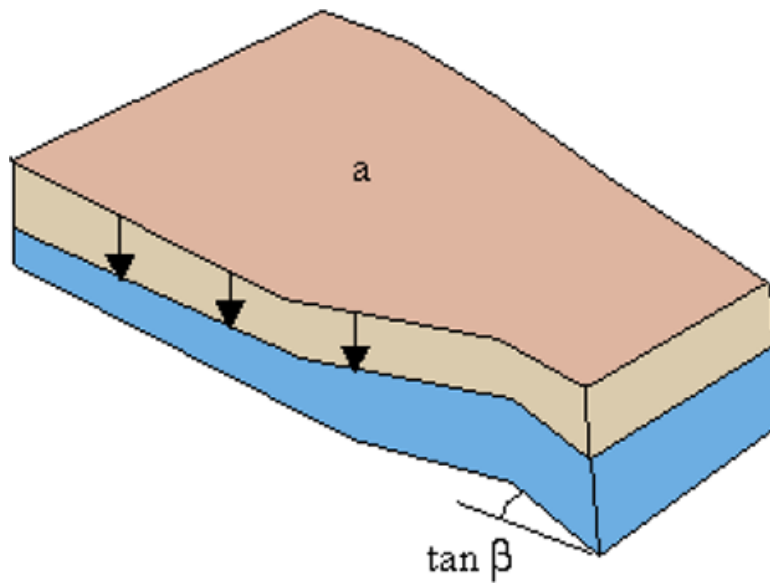


Fig. 3. Determination of the Kirkby's topographic index.

854

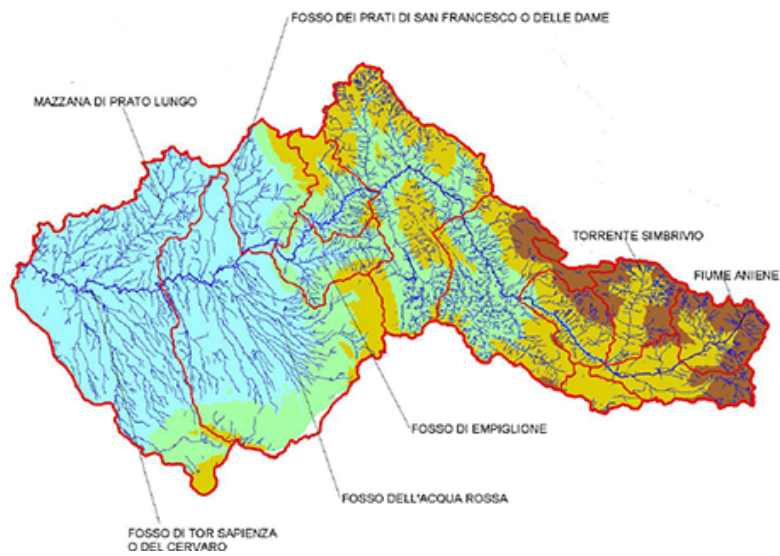


Fig. 4. Hydrographs and altimetry for Aniene River.

855

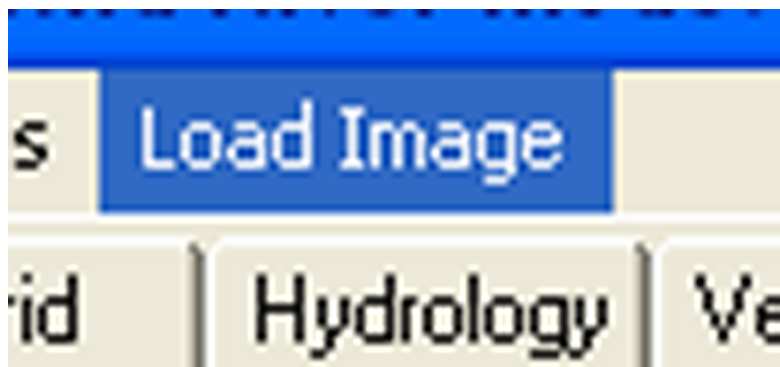


Fig. 5. Main menu path.

856

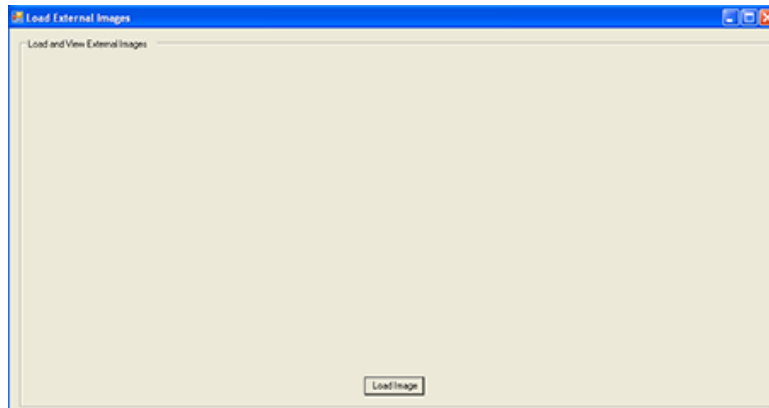


Fig. 6. Load new image in an empty window.

857

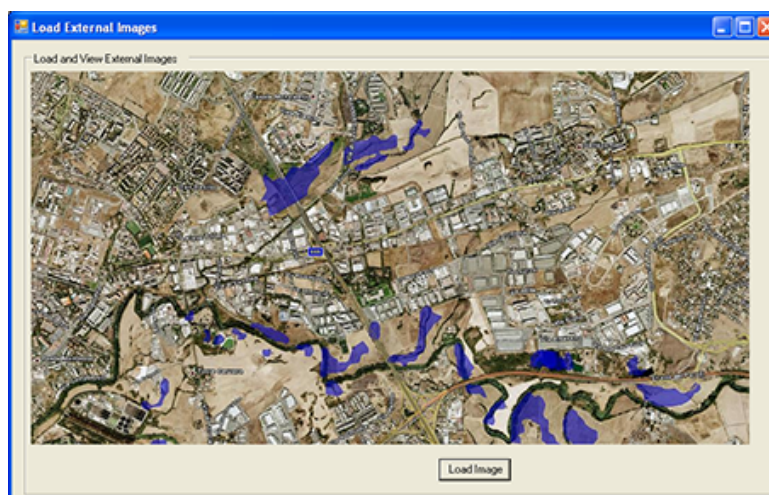


Fig. 7. Sample imported image.

858



Fig. 8. (A) Specular reflection from flooded areas; (B) diffuse reflection from non-flooded area.

859

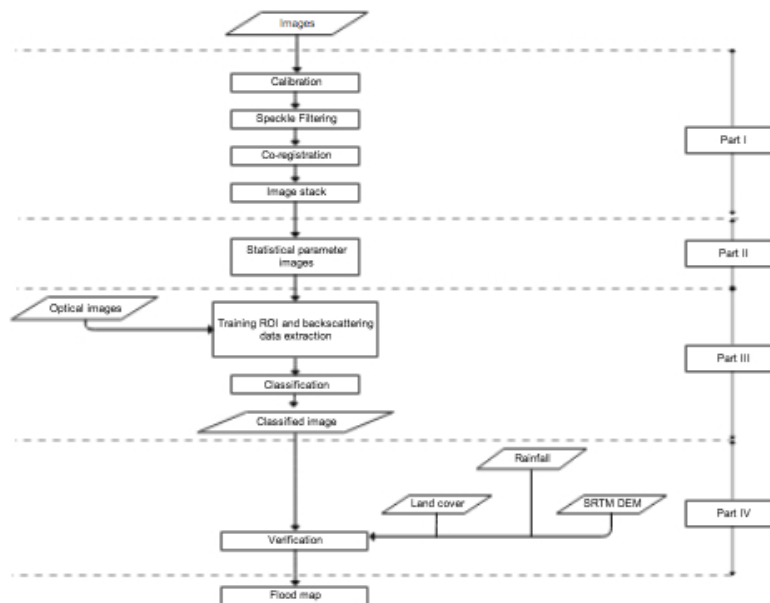


Fig. 9. Flow chart of the flooded area extraction.

860